Supporting Information

Design and Synthesis of Reduced Graphene Oxide/Patronite Composite with Enhanced Lithium-Ion Storage Performance

Yanxia Liu[a], Qiuchen Xu[a], Ran Wang[a], Yiteng Zheng[,b], Zhen Wang[c] and Wenjun Zheng*[,a,d]*

[a]Department of Chemistry, Key Laboratory of Advanced Energy Materials Chemistry (MOE), TKL of Metal and Molecule-based Material Chemistry, College of Chemistry, Nankai University, Tianjin, 300071, P. R. China.

[b]Department of Chemical Engineering and Materials Science, Stevens Institute of Technology, Hoboken, New Jersey 07030, United States.

[c]Key Laboratory of Materials Processing and Mold (Zhengzhou University), Ministry of Education, Zhengzhou University, Zhengzhou 450002, P. R. China.

[d]Collaborative Innovation Center of Chemical Science and Engineering, Nankai University, Tianjin, 300071, P. R. China.

*Corresponding author E-mail: zhwj@nankai.edu.cn; yzheng3@stevens.edu

The formation mechanism analysis of VS_4

It reveals that pure phase of VS_4 is successfully achieved via a facile hydrothermal method by reacting two common raw materials of $Na_3VO_4{\cdot}12H_2O$ and TAA at 160 °C for 24 h, wherein the ratio of S/V is as high as 20. For the reaction procedure, TAA not only acts as the sulfide source but also as a robust reductant. As is well known, the aqueous solution of TAA is weakly alkaline (pH~9),[1] which will hydrolyze completely to form acetate, ammonium and hydrogen sulfide (HS^-), as shown in equation (1).[2]

$$CH_3CSNH_2 + 2\ OH^- \rightarrow CH_3COO^- + NH_3 + HS^- \quad (1)$$

Then, the generated HS^- can be oxidized into $HS^{\cdot}$ under alkaline conditions, furthermore, $HS^{\cdot}$ can continue to form disulfur dianion (S_2^{2-}), which finally react with VO_4^{3-} to generate VS_4, the detailed equations are as follows:[3,4]

$$HS^- \rightarrow HS^{\cdot} + e^- \quad (2)$$

$$HS^{\cdot} \leftrightarrow S^{\cdot -} + H^+ \quad (3)$$

$$2\ S^{\cdot -} \rightarrow S_2^{2-} \quad (4)$$

$$10\ VO_4^{3-} + 21\ S_2^{2-} + 34\ H_2O \rightarrow 10\ VS_4 + 2\ SO_3^{2-} + 68\ OH^- \quad (5)$$

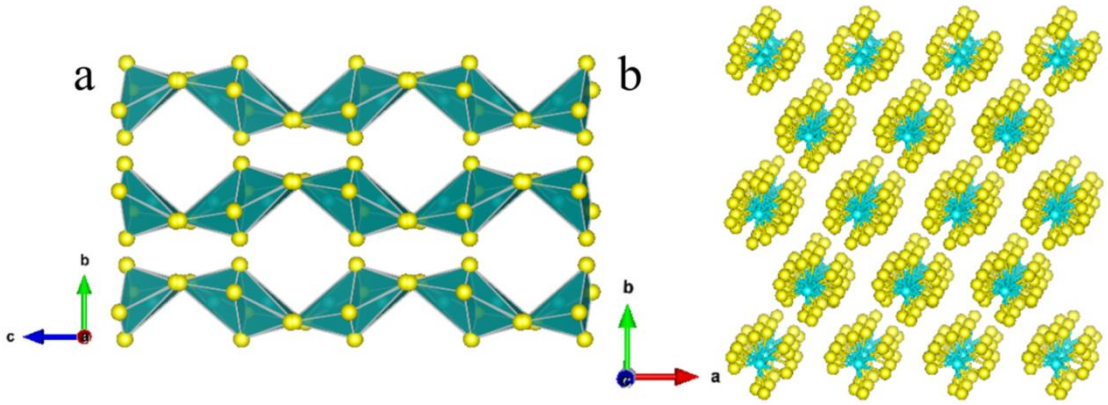

Figure S1. Crystal structure of a linear chain of VS_4. (a) side view along the a axial direction and (b) perspective view along the c axial direction. The yellow balls are S atoms, and the turquoise balls are V atoms.

Figure S2. Structure of 1-butyl-3-methylimidazolium chloride ([BMIm]Cl).

Figure S3. Structure of 1-butyl-3-methylimidazolium acetate ([BMIm]Ac).

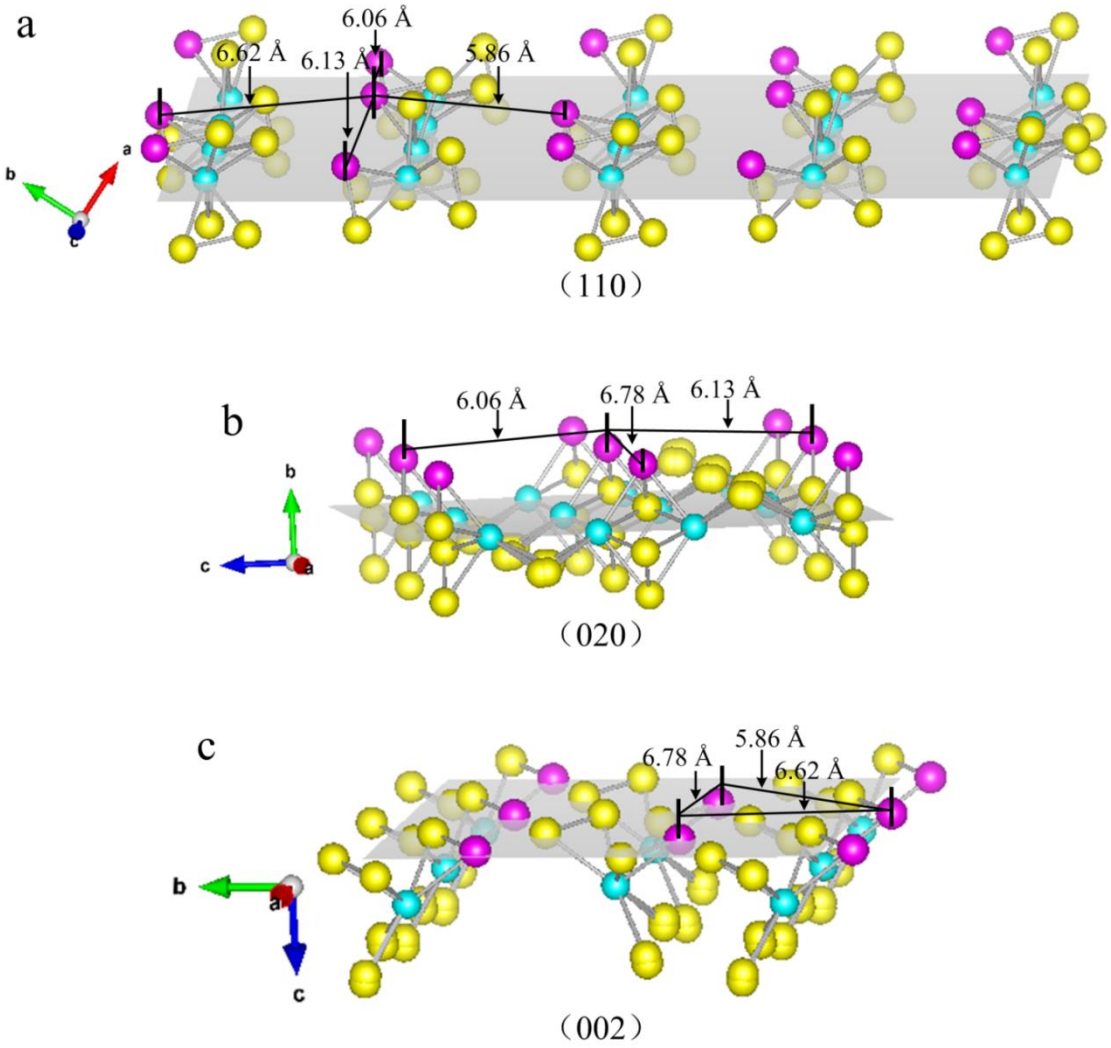

Figure S4. Distances between the adsorption sites of S atoms for the typical crystal surfaces of VS_4: (a) (110) plane, (b) (020) plane and (c) (002) plane.

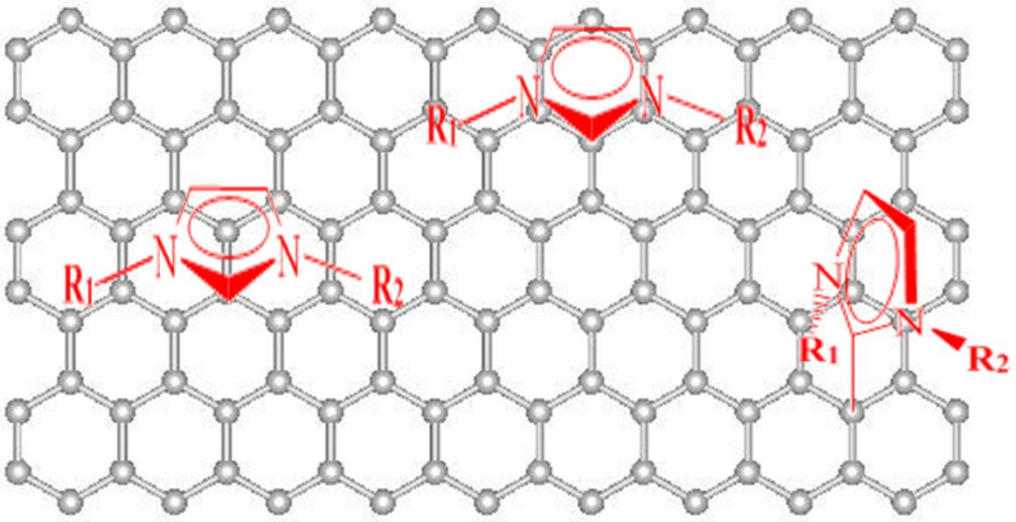

Figure S5. The adsorption configurations between aromatic hydrocarbon molecules and graphene.

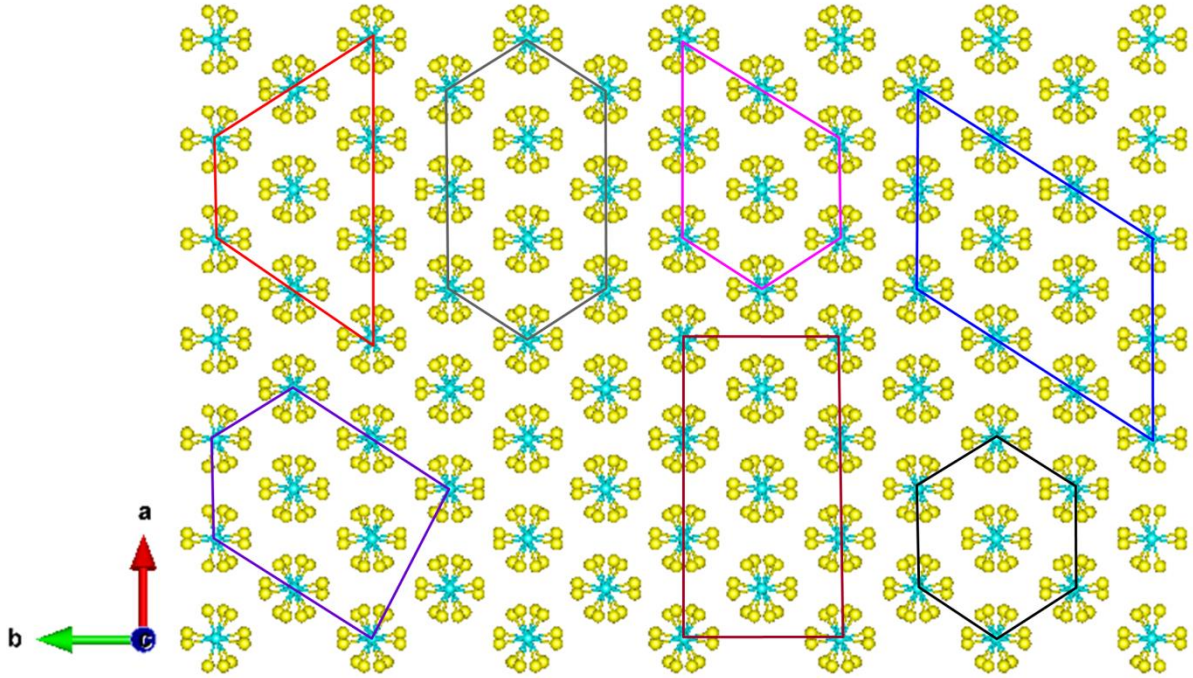

Figure S6. Schematics of the adsorption sites of the several directions of VS_4 chains meeting the requirements of π−π stacking distance of imidazole rings.

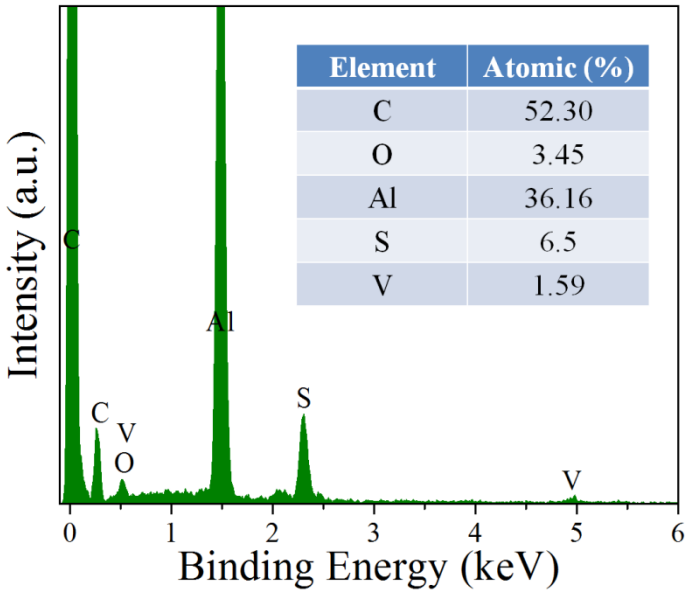

Figure S7. EDS spectrum of the rGO/VS_4 NPs composite (The Al, O and partial C signals stems from Al foil, adsorbed water and conductive tape, respectively).

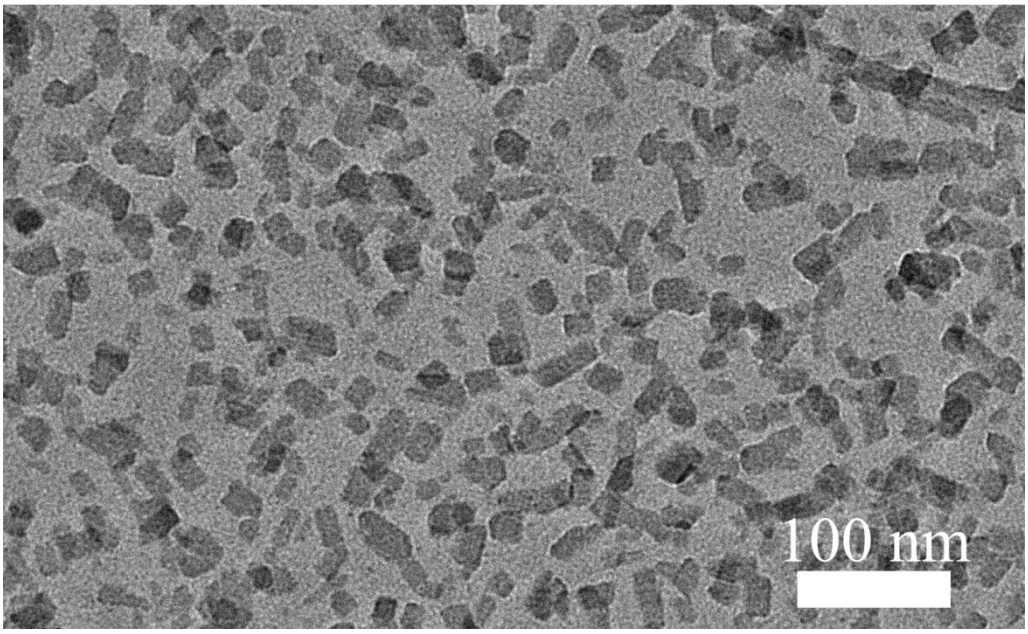

Figure S8. High-magnification TEM image of the rGO/VS_4 NPs composite.

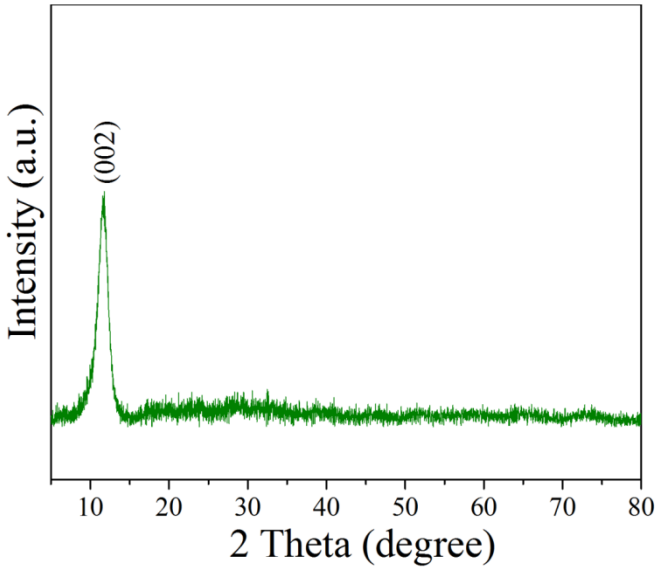

Figure S9. XRD pattern of GO.

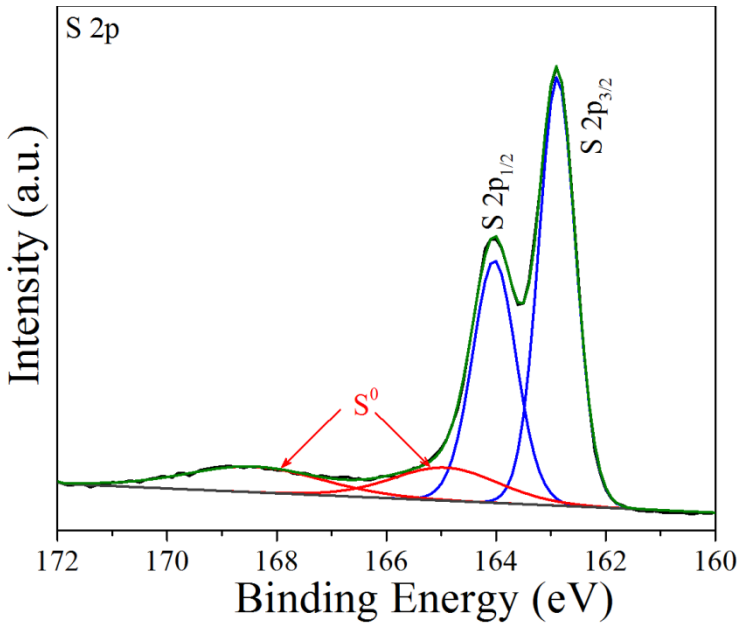

Figure S10. S 2p high-resolution XPS spectrum of the rGO/VS_4 NPs composite.

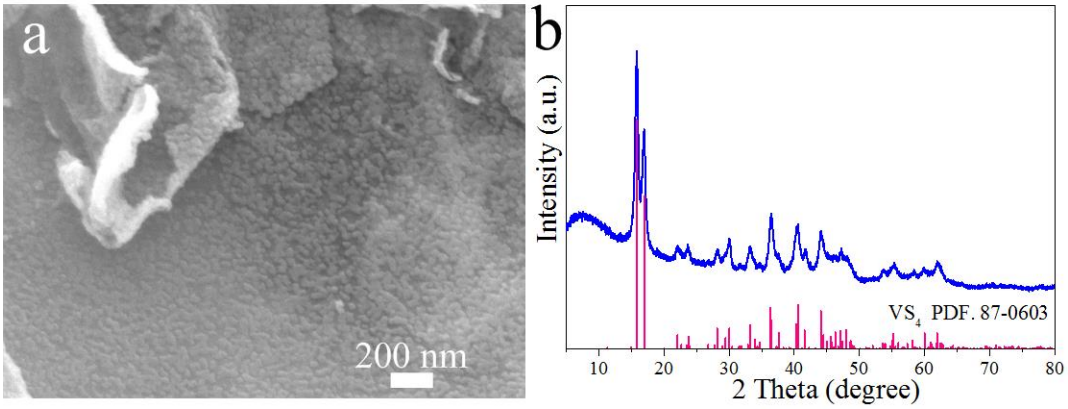

Figure S11. FESEM image (a) and XRD pattern (b) of the product by applying 2 mmol of [BMIm]Ac instead of [BMIm]Cl.

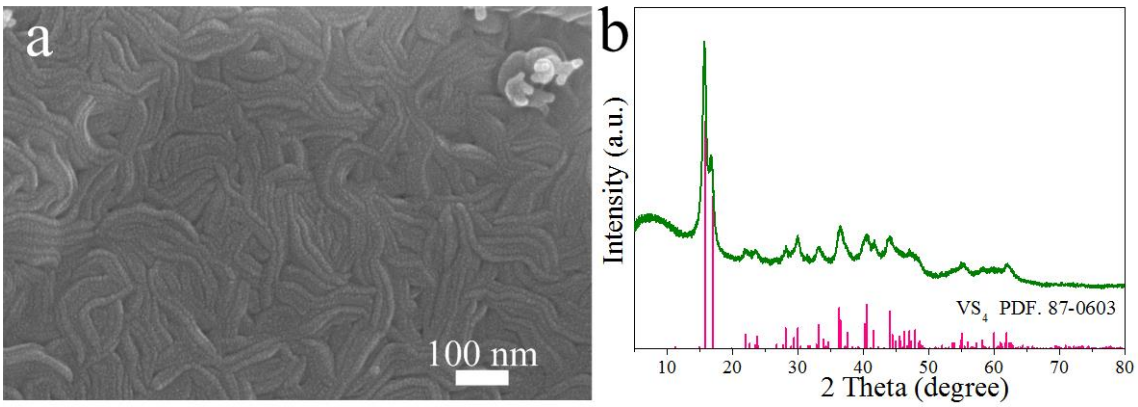

Figure S12. FESEM image (a) and XRD pattern (b) of the product by using 2 mmol of NaCl instead of [BMIm]Cl.

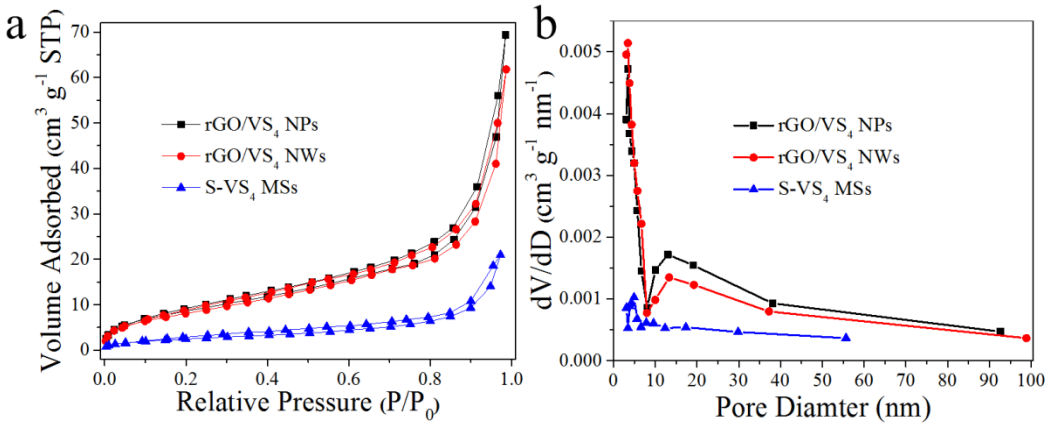

Figure S13. (a) N_2 adsorption−desorption isotherms and (b) the corresponding pore diameter distribution plots of the rGO/VS_4 NPs, rGO/VS_4 NWs and S-VS_4 MSs.

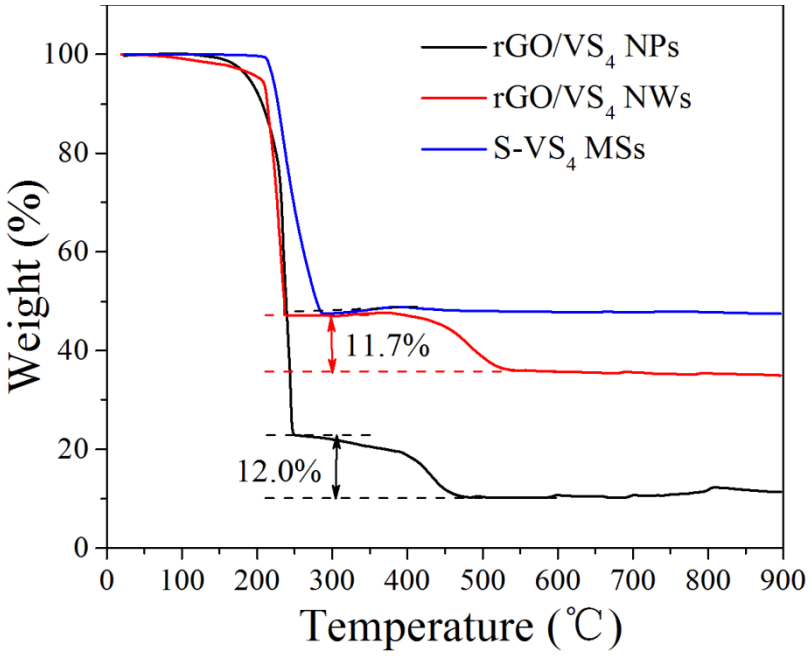

Figure S14. TG curves for the rGO/VS_4 NPs, rGO/VS_4 NWs and S-VS_4 MSs between room temperature and 800 °C in air.

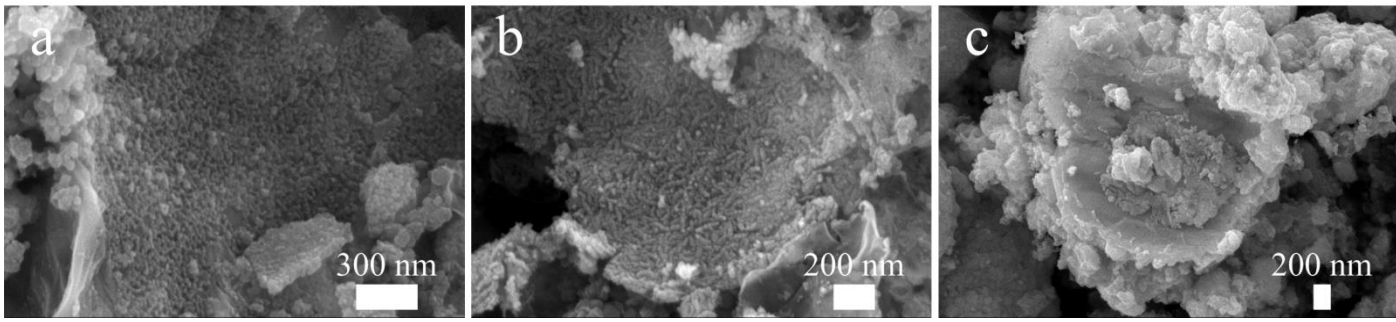

Figure S15. FESEM images of rGO/VS_4 NPs, rGO/VS_4 NWs and S-VS_4 MSs after 240 cycles at 1 A g^{-1}.

Table S1. Parameters obtained from fitting EIS data of the three kinds of anodes (S-VS_4 MSs, rGO/VS_4 NWs and rGO/VS_4 NPs).

Sample	R_s (Ω)	R_{ct} (Ω)
S-VS_4 MSs	4.35	342.2
rGO/VS_4 NWs	3.83	159.6
rGO/VS_4 NPs	3.26	116.5

References

(1) J. Feng, X. Sun, C. Wu, L. Peng, C. Lin, S. Hu, J. Yang and Y. Xie, J. Am. Chem. Soc., 2011, 133, 17832-17838.

(2) E. A. Butler, D. G. Peters and E. H. Swift, Anal. Chem., 1958, 30, 1379-1383.

(3) R. Steudel, Ind. Eng. Chem. Res., 1996, 35, 1417-1423.

(4) G. Lui, G. Jiang, A. Duan, J. Broughton, J. Zhang, M. W. Fowler and A. Yu, Ind. Eng. Chem. Res., 2015, 54, 2682-2689.